Dispersion in stacked-membrane chromatography

Douglas D. Frey, Robert Van de Water and Beibing Zhang

Department of Chemical Engineering, Yale University, New Haven, CT 06520 (USA)

ABSTRACT

A study was conducted of the separation efficiency of a chromatography column consisting of layers of porous polyvinyl chloride membranes incorporating submicron silica particles. It was determined that dispersion inside the membrane was the dominant band-broadening mechanism under most conditions. Experimental data are discussed and compared with previous work.

INTRODUCTION

Conventional chromatography columns containing porous particles suffer from several deficiencies which hamper their large-scale use. Chief among these is the fact that high mass-transfer efficiencies are most readily achieved through the use of small particles, which in turn leads to high operating pressures and large capital costs. To circumvent this difficulty, a variety of novel chromatographic processes have been considered in which high efficiencies and low operating pressures are potentially achieved. Examples include aligned-fiber columns [1], columns employing bundles of hollow fibers [2,3], and columns composed of layers of flat porous membranes [4–6].

The purpose of this study was to investigate the separation efficiency of a commercial stacked-membrane chromatography column. Several previous investigations have demonstrated the usefulness of these columns for biomolecule separations. In particular, Piotrowski and Scholla [4] have shown that stacked-membrane columns incorporating submicron silica particles can attain adsorption capacities in the range required for preparative chromatography. However, previous investigations of these columns have not included systematic measurements of column efficiency.

EXPERIMENTAL

Fig. 1 illustrates the construction of the stacked-membrane columns used in this study. The columns were provided by Kontes Life Science Products and
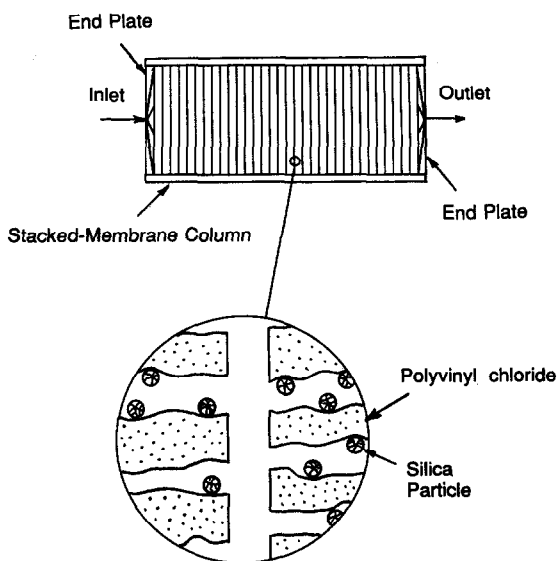

Fig. 1. Construction of a stacked-membrane chromatography column.

Correspondence to: Dr. D. D. Frey, Department of Chemical Engineering, Yale University, New Haven, CT 06520, USA.

consisted of layers of polyvinyl chloride membranes (MPS Microporous Sheets, FMC) having a thickness of 600 μm and a diameter of 2.5 cm. The majority of the adsorption capacity of the column is provided by submicron silica particles embedded in the membrane. For the columns used in this study, the silica particles and polyvinyl chloride membranes were coated with polyethyleneimine such that the columns could be used for anion-exchange chromatography. Columns having lengths of 1 and 5 cm were employed. The columns were housed in a plastic cylinder and were connected to PTFE tubing using "high-resolution" end plates supplied by the column manufacturer.

Standard laboratory procedures and chromatographic equipment were used to evaluate the columns. The solvent used in all the experiments was 50 mM phosphate buffer, pH 7, which had been passed through a 0.45-μm nylon filter. The tubing used was 1/16 in. (0.16 cm) O.D. and was composed of PTFE. A solvent pump (Model RP-SY with a Model RH1CKC pump head, Fluid Metering) and pulse dampener (Model PD-60-LF, Fluid Metering) were used to deliver the solvent to the column. Feed slugs were injected into the membrane column using a six-port sample injection valve (Model 7010, Rheodyne). The effluent from the column passed through a variable-wavelength UV detector (Model LC-85, Perkin Elmer) which was set to either 210 or 254 nm. The signal from the detector was stored and processed on an AT-class microcomputer using an IBM data acquisition and control adapter board.

The first absolute (μ_1) and second central (μ_2) moments of the effluent concentration profiles were determined by numerical integration as follows:

$$\mu_1 = \frac{\sum_{i=1}^{n} t_i C(t_i)}{\sum_{i=1}^{n} C(t_i)} \tag{1}$$

$$\mu_2 = \frac{\sum_{i=1}^{n} (t_i - \mu_1)^2 C(t_i)}{\sum_{i=1}^{n} C(t_i)} \tag{2}$$

where $C(t_i)$ denotes the solute concentration in the effluent for data point i and n is the total number of data points.

THEORY

For a membrane column incorporating silica particles, the second central moment of the effluent concentration profile which results from the injection of a feed slug of width t_{feed}, is given by eqn. 3 [7]:

$$\mu_{2,\text{total}} = \mu_{2,\text{dispersion}} + \mu_{2,\text{extra}} + \mu_{2,\text{fluid}} +$$
$$\mu_{2,\text{particle}} + t_{\text{feed}}^2/12 \tag{3}$$

The terms $\mu_{2,\text{dispersion}}$, $\mu_{2,\text{extra}}$, $\mu_{2,\text{fluid}}$, and $\mu_{2,\text{particle}}$ in eqn. 3 account, respectively, for band broadening from fluid velocity variations in the column, extra-column effects, mass transfer from the mobile liquid filling the membrane pores to the silica particles, and diffusion in the pores of the silica particles. Eqn. 3 ignores the kinetics for surface adsorption and axial molecular diffusion since they are both negligible compared to other mechanisms for band spreading in ion-exchange chromatography. Each term on the right side of eqn. 3 can be divided by the square of the average retention time (i.e., μ_1^2) and multiplied by the column length to yield the corresponding plate height increment. The total plate height (H) resulting from the broadening mechanisms inside the column is therefore given by:

$$H = H_{\text{fluid}} + H_{\text{particle}} + H_{\text{dispersion}} \tag{4}$$

If the entire adsorption capacity of the column results from adsorption in the silica particles, then the equations describing band broadening for chromatography [7] lead to the following expressions for H_{particle} and H_{fluid}:

$$H_{\text{particle}} = \frac{d_p^2 \tau(1-\alpha)v}{30 D \varepsilon \alpha} \frac{\lambda^2}{(1+\lambda)^2} \tag{5}$$

$$H_{\text{fluid}} = \frac{2v}{k_1 a} \frac{\lambda^2}{(1+\lambda)^2} \tag{6}$$

where d_p is the average diameter of the silica particles, k_1 is the coefficient for mass transfer between the liquid in the membrane pores and the silica particles, a is the corresponding area per unit volume, and λ is the ratio of the amount of adsorbate within the exterior surface of the silica particles to the amount of adsorbate in the membrane pores per unit volume of bed. The quantity λ is therefore given by

$$\lambda = k'\left(\frac{\alpha + \varepsilon\sigma}{\alpha}\right) + \frac{\varepsilon\sigma}{\alpha} \tag{7}$$

where α is the volume fraction of mobile fluid in the membrane, σ is the volume fraction of silica particles in the column, and ε is the void fraction in the silica particles. The equilibrium parameter k' in eqn. 7 is defined as

$$k' \equiv \frac{t_R - t_0}{t_0} = K_{eq}\frac{\sigma(1 - \varepsilon)}{\alpha + \varepsilon\sigma} \qquad (8)$$

where t_R is the retention time of the solute in the column, t_0 is the retention time of a solute which has access to the entire pore network but which does not interact with the sorbent surface, and K_{eq} is the adsorption equilibrium constant defined as the amount of adsorbed solute per unit volume of silica divided by the solute concentration in the bulk solution at equilibrium. The retention time in the column is related to the superficial velocity (v_s) by the relation:

$$t_R = (\alpha + \varepsilon\sigma)(1 + k')L/v_s \qquad (9)$$

RESULTS AND DISCUSSION

Scanning electron microphotographs of the membranes used in this study indicated that the membrane pores are highly tortuous and have a wide size distribution. The majority of the pores appeared to have diameters between 1.0 and 5.0 μm. The pore size which would yield a solute velocity equal to the average solute velocity in the membrane can be determined from the membrane permeability using the Hagen–Poiseuille law as follows [8]:

$$d_{pore} = \sqrt{\frac{32\,BT}{\alpha}} \qquad (10)$$

In eqn. 10, B is the Darcy's law permeability given by the quantity $v_s\,\mu L/\Delta P$ and T is the average length of the flow path in the membrane divided by the membrane thickness. In order to use eqn. 10, an approximation for T is required. According to Dullien [9], a volume-average pore diameter for a bed of unconsolidated spheres can be estimated by equating the pore area per unit total volume for a medium containing cylindrical pores to the same ratio for a bed of spherical particles, i.e., $4\alpha/d_{pore} = 6(1 - \alpha)/d_p$ where d_p is the diameter of a spherical particle. If this relation is used to eliminate d_{pore} and introduce d_p into eqn. 10, then that equation becomes equivalent to the Karmen–Kozeny equation

[10] if $T = 2.1$, which will be the value for T assumed here. The Darcy's law permeability of the membrane columns was measured to be $8.3 \cdot 10^{-10}$ cm^2. The void fraction was measured to be 0.60 by weighing a column when it was full of buffer and weighing it again after complete drying in a desiccator. A similar value for the void fraction was obtained using eqn. 9 and measuring the retention time for urea, which is presumably unadsorbed under the conditions used. In both determinations the product $\varepsilon\sigma$ was assumed small compared to α. From these measurements it follows from eqn. 10 that $d_{pore} = 3.0$ μm.

If properties characteristic of the membranes used in this study are substituted into eqns. 4–8 (e.g., $d_{pore} = 3 \cdot 10^{-4}$ cm, $\tau = 10$, $d_p = 5 \cdot 10^{-4}$ cm, $\alpha = 0.60$, $\sigma = 0.2$, $\varepsilon = 0.4$) and if the mass-transfer correlation of Wilson and Geankoplis [11] is employed to predict k_1 [i.e., $k_1 = 0.83\,D^{2/3}v^{1/3}(1 - \alpha)^{-2/3}d_{pore}^{-2/3}$ and $a = 6\,\sigma d_p^{-1}$], the resulting values of H_{fluid} and $H_{particle}$ for strongly adsorbed solutes ($k' > 1$) are at least two orders of magnitude smaller than the experimentally observed second central moment. For this reason, this section considers the evaluation of the term $H_{dispersion}$ in eqn. 4, which largely determines the overall column efficiency. In order to investigate $H_{dispersion}$ as accurately as possible, experimental conditions were chosen so that very little adsorption occurred, i.e., $k' \ll 1$. In particular, the basic protein cytochrome c and the amino acid tryptophan were used together with a 50 mM phosphate buffer at pH 7. Under these conditions k' was 0.1 for the former solute and 0.2 for the latter solute while H_{fluid} and $H_{particle}$ as determined by eqns. 4–8 were in both cases at least three orders of magnitude smaller than the experimentally observed second central moment.

Fig. 2 shows measurements of extra-column band broadening at several flow-rates. These experiments were performed by removing the column from the end plates and replacing it with a thin, solid PTFE disk with the same diameter as the column and with 24 holes drilled through it around the periphery. The response to an injection of benzoic acid was then measured and the value $t_{feed}^2/12$ was subtracted from the result. As shown in Fig. 2, $\mu_{2,extra}$ is a linear function of v_s^{-2} which implies that when a column is inserted between the end plates, H_{extra} will be independent of v_s.

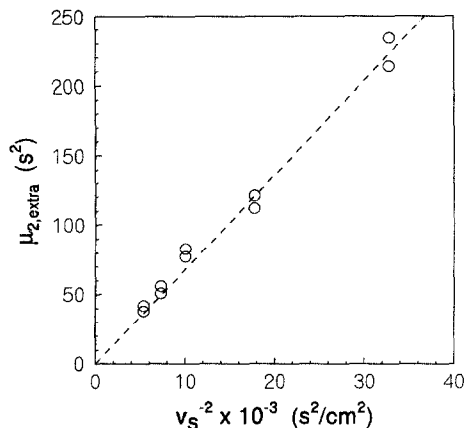Plate height measurements for tryptophan and

Fig. 2. Extra-column band broadening measured by replacing membrane column with thin insert.

cytochrome c for both 1- and 5-cm columns are shown in Fig. 3. The plate height in Fig. 3 was determined by subtracting from the experimentally measured second central moment the sum of $t_{feed}^2/12$ and $\mu_{2,extra}$ from Fig. 2, multiplying that difference by the ratio of the column length to the square of the average retention time in the column, and then non-dimensionalizing the result using the pore diameter from eqn. 10 (left vertical axis) and the membrane thickness (right vertical axis). The interstitial velocity in Fig. 3 is non-dimensionalized using the pore diameter and solute diffusivity. The major sources of experimental error in these measurements appear to be the uncertainty introduced by the signal
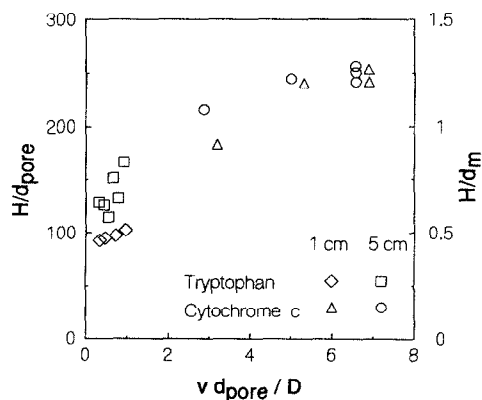

Fig. 3. Reduced plate height as a function of the reduced velocity for 1- and 5-cm columns. $d_{pore} = 3.0$ μm, $d_m = 600$ μm.

noise when determining the baseline and the uncertainty introduced by subtracting $\mu_{2,extra}$ as determined from Fig. 2 from the measured second moment.

The plate height measurements for the 5-cm column appear to be the more reliable of the data sets shown in Fig. 3 since $\mu_{2,extra}$ is insignificant for a column of that length. As shown in Fig. 3, the plate height for the 5-cm column increases from a minimum of 150 pore diameters to a maximum of 240 pore diameters as the flow-rate increases. As mentioned earlier, plate heights for the membrane columns are three orders of magnitude larger than the sum of H_{fluid} and $H_{particle}$ as predicted by eqns. 5–8. This indicates that mass transfer from the membrane pores to the silica particles does not play a significant role in these experiments. Instead, axial dispersion is the dominant band-broadening mechanism and any increase in plate height with flow-rate is likely due to the coupling which generally exists between molecular diffusion and axial dispersion [7].

The data in Fig. 3 can be compared to results for a packed bed of non-porous spheres where, depending on the method used to pack the bed, the plate height increases from a minimum at low flow-rates which is between 2 and 6 pore diameters to a maximum at high flow-rates which is between 4 and 40 pore diameters [12–14]. In accordance with the earlier discussion of the relation between d_{pore} and d_p, these results assume that the average pore size is approximately $d_p/2$ for a bed of randomly packed spheres (i.e., when $\alpha \approx 0.35$). The larger values of $H_{dispersion}/d_{pore}$ observed for membranes are apparently due to the reduced degree to which the membrane pores are interconnected as compared to the pores of a particulate bed. This permits a convective velocity bias for a particular solute molecule to persist for a much larger number of pore diameters. Nevertheless, in spite of the limited degree to which the membrane pores are apparently interconnected, individual pores contact each other often enough such that an increase in the solute diffusivity decreases the distance that a convective velocity bias is maintained for a particular solute molecule.

Fig. 3 indicates that as few as one theoretical plate is observed per membrane. This suggests that the residence time distribution for an unadsorbed solute in an individual membrane is very broad, reaches a

maximum at relatively small residence times, and approaches zero at large residence times very slowly (*i.e.*, the distribution has a significant tail at large times), since distributions having these characteristics correspond to a number of theoretical plates near unity.

Finally, Fig. 3 can be compared to results reported recently by Briefs and Kula [6]. Those workers investigated a stack of 97 nylon-based membranes having a total thickness of 1.7 cm and a Darcy's law permeability of $3.4 \cdot 10^{-10}$ cm² which, according to eqn. 10, yields an average pore size of 1.9 μm. Fig. 8 from Briefs and Kula [6] illustrates the response to a step change in influent concentration as compared to theoretical calculations for the case where axial dispersion is the dominant band-spreading mechanism. If the tailing shown in the figure is ignored, the figure indicates that the effective axial dispersion coefficient is between $5 \cdot 10^{-8}$ and $1 \cdot 10^{-7}$ m² s⁻¹ for a superficial flow-rate of 4 cm/min. Since the corresponding value of $H_{\text{dispersion}}$ is given by the quantity $2 D_{\text{axial}}/v$ (see ref. 7), this implies that $H_{\text{dispersion}}/d_{\text{pore}}$ and $H_{\text{dispersion}}/d_{\text{m}}$ as measured by Briefs and Kula [6] are between 50 and 100 and between 0.52 and 1.04, respectively, which are both comparable to the values obtained in this study.

SYMBOLS

a	area per unit volume, cm⁻¹
B	Darcy's law permeability, cm²
D	diffusion coefficient in mobile phase, cm² s⁻¹
D_{axial}	axial dispersion coefficient, cm² s⁻¹
d_{m}	membrane thickness, cm
d_{p}	particle diameter or silica particle diameter, cm
d_{pore}	pore diameter, cm
H	height of theoretical plate, cm
K_{eq}	equilibrium constant
k'	equilibrium parameter
k_1	mass-transfer coefficient, cm s⁻¹
L	column length, cm
N	number of theoretical plates
ΔP	pressure drop across column, g cm⁻¹ s⁻²
T	empirical ratio between pore length and membrane thickness
t_0	retention time for an unsorbed solute, s
t_{feed}	size of solute injection slug, s
t_{R}	retention time for a solute in the column, s

v	interstitial fluid velocity, cm s⁻¹
v_{s}	superficial fluid velocity, cm s⁻¹

Greek symbols

α	volume fraction occupied by mobile fluid in membrane
ε	porosity of silica particles
λ	equilibrium constant defined in eqn. 7
μ	viscosity, g cm⁻¹ s⁻¹
μ_1	first absolute moment, s
μ_2	second central moment, s²
σ	volume fraction of silica particles
τ	diffusional tortuosity

ACKNOWLEDGEMENTS

REFERENCES

1 R. Hegedus, *J. Chromatogr. Sci.*, 26 (1988) 425.
2 S. Brandt, R. A. Goffe, S. B. Kessler, J. L. O'Connor and S. E. Zale, *Bio/Technology*, 6 (1988) 779.
3 H. Ding, M.-C. Yang, D. Schisla and E. L. Cussler, *AIChE J.*, 35 (1989) 814.
4 J. J. Piotrowski and M. H. Scholla, *BioChromatography*, 3 (1988) 161.
5 *MemSep Chromatography Cartridge Technical Bulletin*, Millipore, Bedford, MA, 1991.
6 K.-G. Briefs and M.-R. Kula, *Chem. Eng. Sci.*, 47 (1992) 141.
7 J. C. Giddings, *Dynamics of Chromatography, Part 1, Principles and Theory*, Marcel Dekker, New York, 1965.
8 R. E. Kesting, *Synthetic Polymer Membranes*, McGraw-Hill, New York, 1971.
9 F. A. L. Dullien, *Porous, Media Fluid Transport and Pore Structure*, Academic Press, New York, 1979.
10 R. B. Bird, W. E. Stewart and E. N. Lightfoot, *Transport Phenomena*, Wiley, New York, 1960.
11 E. J. Wilson and C. J. Geankoplis, *Ind. Eng. Chem. Fundam.*, 5 (1966) 9.
12 Cs. Horváth and H.-J. Lin, *J. Chromatogr.*, 126 (1976) 401.
13 P. Magnico and M. Martin, *J. Chromatogr.*, 517 (1991) 31.
14 S. F. Miller and C. J. King, *AIChE J.*, 12 (1966) 767.